N94- 35909

CONCEPTS OF FLYWHEELS FOR ENERGY STORAGE USING AUTOSTABLE HIGH-T_C SUPERCONDUCTING MAGNETIC BEARINGS

H. J. Bornemann, R. Zabka, P. Boegler, C. Urban and H. Rietschel
Kernforschungszentrum Karlsruhe GmbH
Institut für Nukleare Festkörperphysik
P.O. Box 3640, D-76021 Karlsruhe, Germany

SUMMARY

A flywheel for energy storage using autostable high-T_C superconducting magnetic bearings has been built. The rotating disk has a total weight of 2.8 kg. The maximum speed is 9240 rpm. A process that allows accelerated, reliable and reproducible production of melt-textured superconducting material used for the bearings has been developed. In order to define optimum configurations for radial and axial bearings, interaction forces in three dimensions and vertical and horizontal stiffness have been measured between superconductors and permanent magnets in different geometries and various shapes. Static as well as dynamic measurements have been performed. Results are being reported and compared to theoretical models.

INTRODUCTION

In times of rapidly increasing energy consumption, facing an impending shortage of natural resources for energy production, the need has arisen for highly efficient, regenerative energy storage systems. Energy can be stored in the form of chemical (e.g. batteries), thermal (e.g. latent heat), electromagnetic and mechanical energy. Applications of mechanical energy storage devices include compressed gas facilities, pumped hydroelectric storage and flywheels. A flywheel stores energy in the form of kinetic (rotational) energy. Whereas each energy storage system has its inherent advantages and disadvantages compared to the others, it is the overall system performance and simplicity of flywheels that make them especially useful for a variety of applications.

With the introduction of magnetic bearings which allow frictionless, non-contact support of a rotating body, the efficiency of flywheels for energy storage for which reduced friction is of crucial importance could be increased consid-

erably. The bearings have been developed over the last years for applications that are exceptionally critical concerning friction and/or wear. In the field of power systems, such applications include, in addition to flywheels, all cold machines for which wear is a considerable problem such as generators, motors and cold compressors.

However, these configurations which involve permanent magnets and coils are intrinsically unstable due to Earnshaw's theorem [1-3]. Therefore, at least one component has to be adjusted continuously. In order to function, these active magnetic bearings require elaborate control systems. The reduction of the complexity and cost of such control systems as well as the increase in reliability of these bearings are still points of major concern in the field.

On the other hand, such drawbacks can be avoided with completely passive autostable magnetic bearings involving superconducting materials combined with permanent magnets. The high-temperature superconductor $YBa_2Cu_3O_7$ (YBCO) looks especially promising because it requires cooling by liquid nitrogen (T=77 K) only. In contrast, conventional superconductors have to be cooled by liquid helium which adds considerable cost and complexity to practical applications.

In small magnetic fields, superconductors can prevent magnetic field penetration absolutely, which is known as the Meissner effect [4]. In this situation a magnet can levitate above a superconductor and vice versa. However, the interaction is relatively weak which limits the range of possible applications. Much stronger levitation forces can be obtained in high magnetic fields, when the superconductor exhibits pinning.

With increasing magnetic field strength H, the field starts to enter the superconductor in the form of magnetic flux bundles. The field where the transition takes place is called the lower critical field H_{c1}. For superconducting YBCO $H_{c1} \approx 100$ Oe at 77 K. Type II superconductors, also called hard superconductors, have the ability to pin those flux lines. Inside the superconductors the flux bundles are shielded by ring currents flowing throughout the volume and the gradient of the magnetic induction B is proportional to the critical current density J_c. The superconductor is in the critical state or Shubnikov phase. It is because of the pinning effect that melt-textured YBCO exhibits considerable levitation forces in high magnetic fields. The dc magnetization M is irreversible over an extended magnetic field range, resulting in a magnetic hysteresis loop. According to Bean's law [5], for a given value of the magnetic field H, the difference in magnetization, M_+-M_-, is proportional to the

critical current density J_c and to the size of the shielding current loop d

$$M_+-M_- \sim J_c \cdot d \qquad (1)$$

Here, M_+ and M_- are magnetization values obtained for the ascending and descending branch of the hysteresis loop, respectively, d is the diameter of the current loop. In one dimension, the levitation force F can be written as

$$F \sim M \cdot V \cdot grad(H) \qquad (2)$$

where V is the volume of the superconductor and grad(H) is the field gradient produced by a magnet. Together with eqn. (1) it follows that large levitation forces are obtained in high magnetic field gradients for superconducting materials that exhibit large values of both the critical current density J_c as well as the size of the shielding current loop d.

In superconducting YBCO J_c is localized in individual grains. Therefore large levitation forces require samples with large grains (large d) which exhibit strong pinning forces (large J_c). Murakami et al. developed the so called MPMG (Melt Powder Melt Growth) process [6] which allows fabrication of well-textured, large grain YBCO samples with large J_c values and strong pinning forces. The material exhibits considerable levitation forces as demonstrated by levitating a person on a disk with 200 Nd-Fe-B magnets embedded (total weight, person+disk was 1100 N) above 200 melt processed YBCO superconducting pellets [7].

We have investigated concepts of flywheels for energy storage using autostable high-temperature superconducting magnetic bearings. Static as well as dynamic interaction forces between melt-textured superconducting materials and permanent magnets have been measured. Results are being reported and compared to theoretical models.

EXPERIMENTS

Samples were prepared using commercially available YBCO powder [8]. The process used is similar to the melt process (Melt-Texture Growth, MTG process) originally devised by Jin et al. [9] and further developed by Salama et al. [10] and by Hojaji et al. [11]. We made the following modifications: Instead of adding Y_2BaCuO_5 to the starting material, we added finely ground Y_2O_3 powder. The first step of the MPMG process - heating to 1400 °C with a subsequent quench - was omitted. In addition to Y_2O_3, Ag_2O was added to avoid the formation of cracks. A detailed descrip-

tion of the process will be published elsewhere. Compared to MPMG, our process is shorter and simpler and therefore it can easily be scaled up to industrial production which requires a direct, reproducible process for sample production on a routine basis.

Pellets were mainly produced in two standard sizes: Small size (ϕ 14 mm, mass $\approx$ 14 g) for control samples to optimize the melt-texture process and large size (ϕ 38 mm, mass $\approx$ 100 g) for levitation force measurements and for applications such as in prototype bearings.

Samples were characterized with respect to macrostructure (e.g. grain size, twin structure, precipitates), microstructure (e.g. grain boundaries, inclusions, defects), critical currents and pinning properties. Characterization in terms of macrostructure was carried out with a polarization microscope. Phase purity was checked on a routine basis by X-ray diffraction. The microstructure was analysed using a high resolution TEM with attached EDX/EELS equipment. Critical shielding currents were determined by dc-SQUID magnetization measurements. Detailed results will be published elsewhere.

In order to optimize the melt-texture process, samples were analysed in terms of their flux trapping capabilities and pinning potential. Pellets of the small standard size (ϕ 14 mm) were cooled in the field of a $Nd_2Fe_{14}B$ magnet (ϕ 25 mm, magnetic field H = 5 kOe at the surface, axial polarization). Then the magnet was removed and the remnant magnetic flux was measured as a function of location across the pellets. The magnetic field sensor (Hall probe) had an active area of 0.2 mm^2. The maximum value of the trapped flux was used as criterion of sample quality. For small standard size pellets the grain size is approximately equal to the sample size. Therefore there is a direct correlation between the maximum value of the trapped flux and levitation force (see eqn. (2)). Although the data have local character only, they were found to be quite useful for evaluation of the sample quality and thus provided important input for optimization of the melt-texture process (e.g. temperature profile, amount of Ag_2O and Y_2O_3) with respect to large levitation forces. Fig. 1 shows the maximum trapped flux as a function of both Ag_2O and Y_2O_3 content for a series of small standard size samples. For this series the optimum is reached for 12.5 wt% Ag_2O and 25 at% Y_2O_3 or 17.5 wt% Ag_2O and 20 at% Y_2O_3.

The pinning potential was deduced from magnetic relaxation measurements in a dc-SQUID on representative pieces of pellets. At T = 77 K, the magnetic field was first ramped to H = 10 kOe and then to H = 0. Then, the remnant magnetic moment ($\approx$ trapped

flux) of the specimen was recorded as a function of time over several hours. These experiments also provide information about the total flux trapped by the specimen and the time rate of change of trapped flux. The latter is of special importance with respect to possible applications of these materials such as in superconducting magnetic bearings or in superconducting permanent magnets. For the bearing, the levitation force is proportional to the magnetization (or trapped flux) of the superconducting material (see eqn.(2)). Flux motion will be associated with dissipation resulting in damping which is unwanted in long term applications such as in a flywheel energy storage device. The total remnant flux ϕ in the specimen was found to change logarithmically over a time interval of 14 hours, i.e.

$$\Delta\phi \approx \ln(t/t_o) \qquad\qquad (3)$$

here t_o is typically taken as the time from stabilization of the magnetic field at H = 0 to the first reading of the SQUID (usually 10 - 20 sec). Assuming that the flux continues to decay according to eqn (3) for times > 14 hours it follows that even after 5 years the specimen retained almost 80 % of the flux originally trapped at t = t_o. For practical applications this means that the superconducting material - adequate cooling provided - can be operated for years without 'recharging'.

Three dimensional interaction forces and vertical and horizontal stiffness have been measured between superconductors and permanent magnets in different geometries and various shapes as a function of relative position. Strain gauges were used for the three geometric axes. Resolution was 10 mN. The permanent magnets were mounted at the end of a tripod and mechanically connected to the force sensors via a gimbal suspension. The superconducting pellets were fixed in a liquid nitrogen dewar and mounted on a x-y-z microslide.

It was found that interaction forces depend upon: (I) distance between magnet and superconductor, (II) field and field gradient produced by the magnet, (III) sample size, (IV) sample quality (grain size, pinning forces), and (V) magnet size. Only magnets which can be approximated by a point dipole were used (the ideal magnetic dipole is a sphere) to ensure that the measured data are compatible to theoretical model calculations. Fig. 2 shows the log-log representation of the levitation force F_z as a function of vertical distance r_z between superconductor and magnet for different sized Nd-Fe-B magnets. Magnet data are summarized in table 1. The superconductor was a large standard size YBCO pellet (ϕ 30 mm).

Three distinct regions can be distinguished in fig. 2. For large distances between magnet and superconductor the correlation between $\log_{10}(F_z)$ and $\log_{10}(r_z)$ is linear with a slope of

approximately -4, i. e. $F_z \sim 1/r_z^4$. The distance r_{zo} where the data deviate from the straight line decreases with decreasing magnet size. We find $r_{zo} \approx 20$ mm for magnet A, $r_{zo} \approx 32$ mm for magnet B and $r_{zo} \approx 50$ mm for magnet C. The positions r_{zo} are approximately equal to the points where the vertical component H_z of the field of magnets A, B and C, respectively, has dropped to H_{c1} (see table 1). With decreasing r_z, F_z increases considerably. Close to the superconductor the dependence of $\log(F_z)$ upon $\log(r_z)$ is linear again with a slope of about -2, i.e. $F_z \sim 1/r_z^4$.

For small magnetic fields ($H < H_{c1} \approx 100$ Oe at 77 K) the interior of the superconducting pellet is completely shielded. By using the image method, the vertical force F_z [N], acting on a magnetic dipole m [A·m^2] levitated at a distance r_z [m] above an infinite superconducting plane in the Meissner state can be calculated as follows [12]

$$F_z(r_z) = k \cdot m^2 / r_z^4 \qquad (4)$$

where k is a constant, $k = 3.75 \times 10^{-8}$ VsA^{-1}m^{-1}. The dashed line in fig. 2 represents a least-squares fit to the experimental data produced by magnet A for $r_z > 20$ mm. In this region the field of the magnet is < 100 Oe. From the fit it was found that $F_z(r_z)$ varies as $1/r_z^{4.4}$, in good agreement with the theoretical prediction given in eqn. (4). The magnetic dipole moment m of the magnet was found to be 0.1 Am^2, compared to a calculated value of 0.08 Am^2 using data specified in table 1. The main reasons for the deviation of the experimental data from theory are not surprising, because (i) the magnet is not a perfect dipole and (ii) the superconductor does not represent an infinite plane.

For smaller r_z, $H > H_{c1}$ and the field starts to penetrate the superconductor. A gradual transition to the critical state takes place. The dash-dotted line in fig. 2 is a least-squares fit to the experimental data obtained for magnet C for $r_z < 5$ mm. We find $F_z \sim 1/r^{1.8}$. Hellman et al.[13] have proposed a model for calculating the vertical force on a magnetic dipole levitated above a superconductor in the critical state. Assuming that flux bundles pass straight through the superconductor, the levitation force is found to scale as $1/r_z^2$ in good agreement with our experimental data.

For a given distance, the levitation force is maximum when the size of the magnet is comparable to the size of the superconducting pellet. On the other hand, when the magnet is much larger compared to the superconducting pellet, the levitation force apparently saturates within the range typical for gaps in magnetic bearings (e < 5 mm). This is shown in the insert of fig. 2. Here the superconductor was a small standard size pellet, ϕ 14 mm).

534

Differences in sample quality, evidenced by levitation force measurements, are shown in fig. 3. Magnet C was used for the measurements. All samples are ϕ 30 mm x 18 mm. In the Meissner phase, all samples are alike. Both levitation force F_z and vertical stiffness K_z, given by $\delta F_z/\delta r_z$, depend upon the magnet only. K_z is typically in the range of several mN/cm. With the transition to the critical state, the difference in sample performance with respect to levitation force and vertical stiffness reflects different pinning capabilities. The sample with the highest levitation force also exhibits the strongest vertical stiffness, $K_z \approx 10$ N/cm for $r_z < 3$ mm.

FLYWHEEL ENERGY STORAGE SYSTEM

An engineering model of a flywheel system with an autostable superconducting magnetic thrust bearing has been built and tested. The system comprises the following components: (1) aluminum flywheel disk, (2) superconducting magnetic thrust bearing consisting of a Nd-Fe-B magnet (integrated into the flywheel disk) and 6 melt-textured YBCO pellets on a sample mounting plate, (3) driving unit including drive shaft with couplings, motor/generator and frequency converter, (4) liquid nitrogen cryostat and (5) mounting structure. The components of the superconducting magnetic bearing are shown in fig. 4. The maximum levitation force was 65 N at zero gap. Vertical stiffness at 1 mm gap was 440 N/cm, lateral stiffness was 130 N/cm. Specifications are summarized in table 2.

Test runs were made with the superconducting magnetic bearing placed in a liquid nitrogen cryostat at ambient pressure. The magnet had a special coating to avoid material deterioration due to moisture collecting on the surface during prolonged experiments. The flywheel disk was driven by a 3 phase asynchronous, 380 V motor/generator connected to a frequency converter. Maximum power was 1.5 kW. A schematic of the flywheel system is shown in fig. 5. During high speed runs the unit was placed in a concrete enclosure measuring 1 x 0.8 x 0.8 m. The maximum speed attained was 9240 rpm. The energy capacity at this speed was calculated to be 1.8 Wh. A summary of technical data is given in table 3.

Obviously this set-up was not optimized for energy efficiency. We encountered quite substantial losses resulting from aerodynamic drag, especially during high speed runs and at lower speeds during extended runs when icing of the flywheel disk had occurred. Nevertheless, this preliminary experiment demonstrated the technology of autostable superconducting magnetic bearings and their application in a flywheel for energy storage. The next step will be to integrate the flywheel system into a vacuum

housing where much higher speeds should be possible. Metal parts in the path of the rotating magnetic field will be avoided to reduce losses from eddy currents due to deviations of the field from perfect rotational symmetry. The superconductors will be placed in a closed liquid nitrogen cryostat made from fiberglass. The same driving unit will be used. The projected speed is 24 000 rpm.

SUMMARY

In summary we have shown that large, good quality, monolithic pieces of superconducting YBCO can be produced on a routine basis using a melt-texture growth process. The material exhibited substantial levitation forces and good long term stability. A passive, superconducting magnetic bearing was built and integrated into a flywheel system. The bearing, though only a thrust bearing by design, provided both vertical as well as lateral stiffness. A 2.8 kg flywheel disk was rotated safely at speeds up to 9240 rpm at ambient pressure. The maximum energy capacity was 1.8 Wh. It can be expected that further refinement of this technology will allow operation of superconducting flywheels in the kWh range. Possible applications range from uninterruptable power supplies for computers to momentum/reaction wheels for spacecrafts.

ACKNOWLEDGEMENTS

REFERENCES

1. S. Earnshaw, *Trans. Cambridge Philos. Soc. 7*, 1882, pp. 97-112.
2. L. Tonks, *Elect. Engineering. 59*, 1940, pp.118-119
3. W. Braunbeck, *Zeitschrift für Physik 112*, 1939, pp. 764-769.
4. W. Meissner and R. Ochsenfeld, *Naturwissenschaften 21*, 1933, pp. 787-788.
5. C. P. Bean, *Phys. Rev. Lett. 8*, 1962, pp. 250-253.
6. M. Murakami, T. Oyama, H. Fujimoto, T. Taguchi, S. Goto, Y. Shiohara, N. Kosizuka, and S. Tanaka, *Jpn. J. Appl. Phys. 29*, 1990, pp. L1991-L1994.
7. M. Murakami, ed.: *Melt Processed High-Temperature Superconductors*, World Scientific, 1992, pp. 9-10
8. Hoechst AG, YBaCO 123 powder grade 2.
9. S. Jin, T. H. Tiefel, R. C. Sherwood, R. B. van Dover, G. W. Kammlott and R. A. Fastnacht, *Phys. Rev. B 37*, 1988, pp. 7850-7858.
10. K. Salama, V. Selvamanickam, L. Gao and K. Sun, *Appl. Phys. Lett. 54*, 1989, pp. 2352-2354.
11. H. Hojaji. K. A. Michael, A. Barkatt, A. N. Thorpe, F. W. Mathew, I. G. Talmy, D. A. Haught and S. Alterescu, *J. Mater. Res. 4*, 1989, pp. 28-36.
12. Z. J. Yang, T. H. Johansen, H. Bratsberg, A. Bhatnagar, *Physica C 197*, 1992, pp. 136-146.
13. F. Hellman, E. M. Gyorgy, D. W. Johnson, Jr., H. M. O'Bryan, and R. C. Sherwood, *J. Appl. Phys. 63*, 1988, pp. 447-450.

Table 1: Specifications of the Nd-Fe-B Magnets
(Direction of Magnetization: Axial)

Magnet		A	B	C
Diameter	mm	7	14	25
Height	mm	6	14	21
Mass	g	2.5	19.6	77.4
Max. Field	kOe	4.2	4.5	5.0
Distance where $H_z < H_{c1}$	mm	18	32	48

Table 2: Superconducting Magnetic Bearing -- Specifications

Magnet:	neodymium-iron-boron with coating
	dimensions: ϕ 90 x ϕ 60 x 15 mm
	weight: 397 g
	polarization: axial
	maximum field: 4 kOe
Superconductors:	6 pellets of melt-textured YBCO
	dimensions: ϕ 30 x 18 mm (pellet)
	weight: 100 g (pellet)

Operating temperature:	77 K (liquid nitrogen)
Maximum levitation force:	65 N
Stiffness at 1mm gap:	
Vertical	440 N/cm
Lateral	130 N/cm

Table 3:   Flywheel -- System Data

Flywheel disk:	$AlMg_3$, ϕ 200 x 30 mm, 2.43 kg + integrated Nd-Fe-B magnet total mass: 2.8 kg allowable tensile stress: 210 N/mm^2 moment of inertia: 0.014 $kg \cdot m^2$
Motor/Generator:	3-phase asynchronous, 380 V, 50 Hz, watercooled dimensions: ϕ 176 x 275 mm maximum torque: 1.2 Nm
Maximum speed: Projected speed: Energy capacity: Maximum power:	9240 rpm 24 000 rpm (in vacuum) 1.8 Wh at maximum speed 12.3 Wh at projected speed 1.5 kW
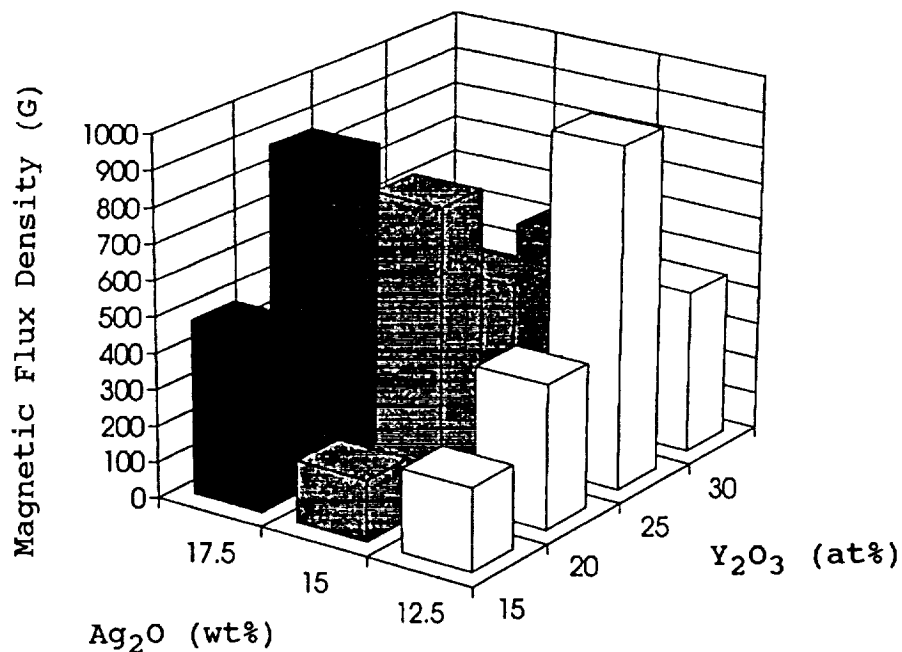
Figure 1: Maximum trapped flux as a function of Ag_2O and
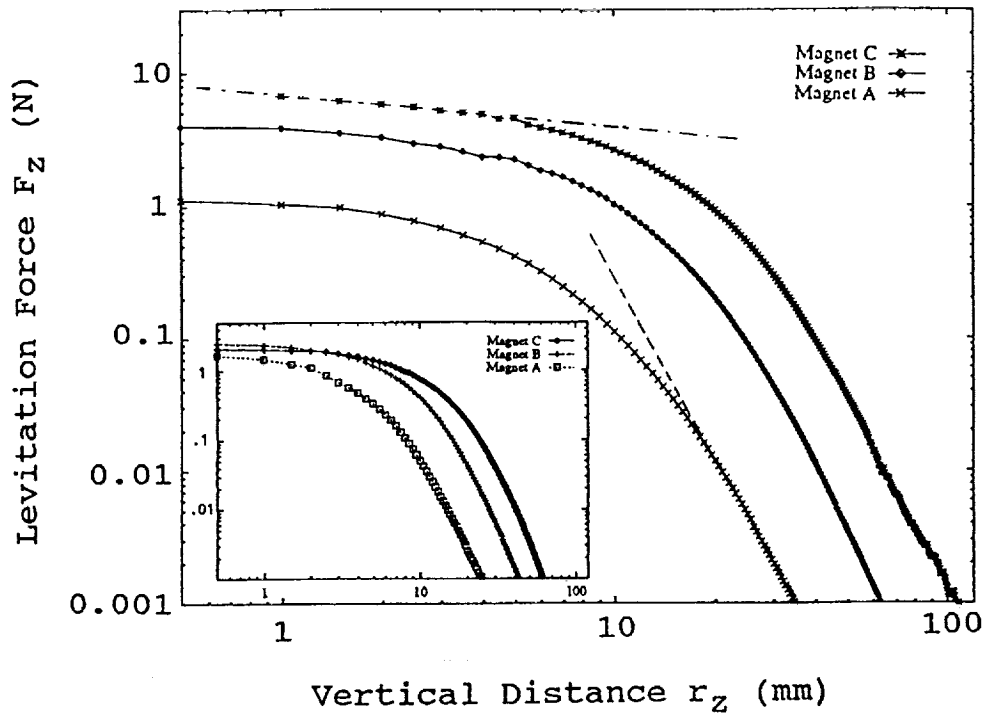Y_2O_3 content for a series of small standard size
pellets (ϕ 14 mm).

Figure 2: Levitation force as a function of vertical distance for different sized magnets. The superconductor was a large standard size pellet (ϕ 30 mm), composition 20 at% Y_2O_3, 15 at% Ag_2O. For the insert: Small standard size (ϕ 14 mm), composition was 20 at% Y_2O_3, 17.5 at% Ag_2O.
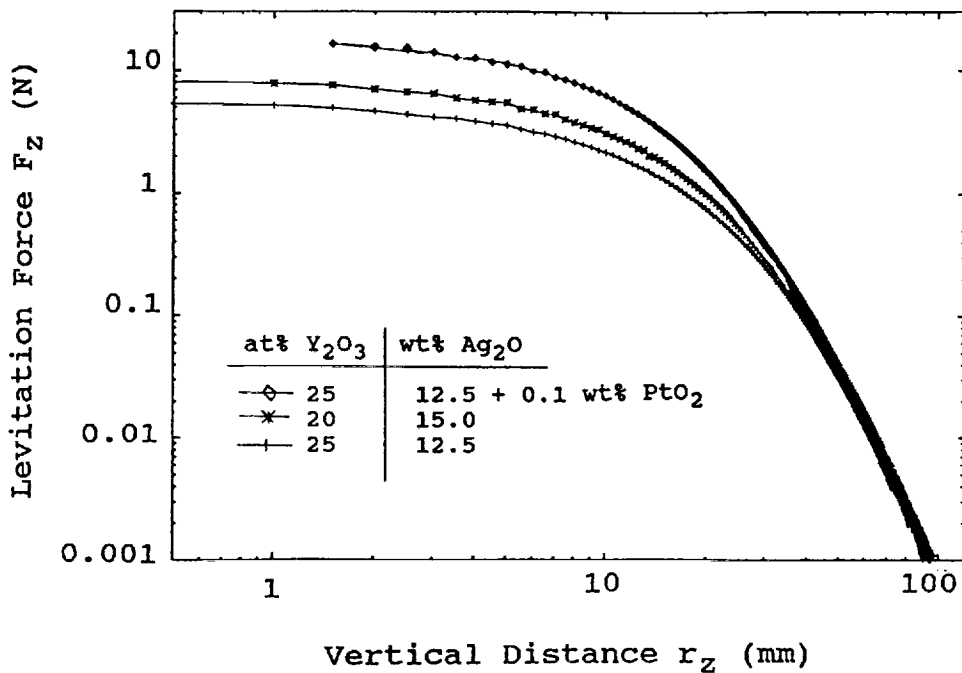

Figure 3: Correlation between levitation force and sample composition.
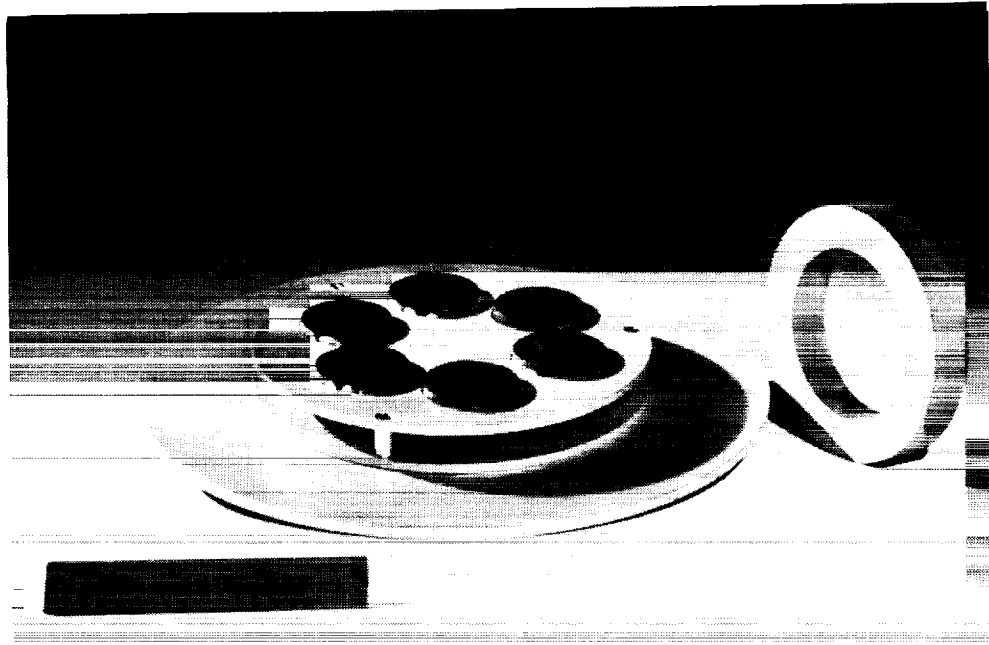
Figure 4: Components of the superconducting magnetic
bearing. Top: Superconducting YBCO pellets
(ϕ 30 x 18 mm) integrated into the sample mounting
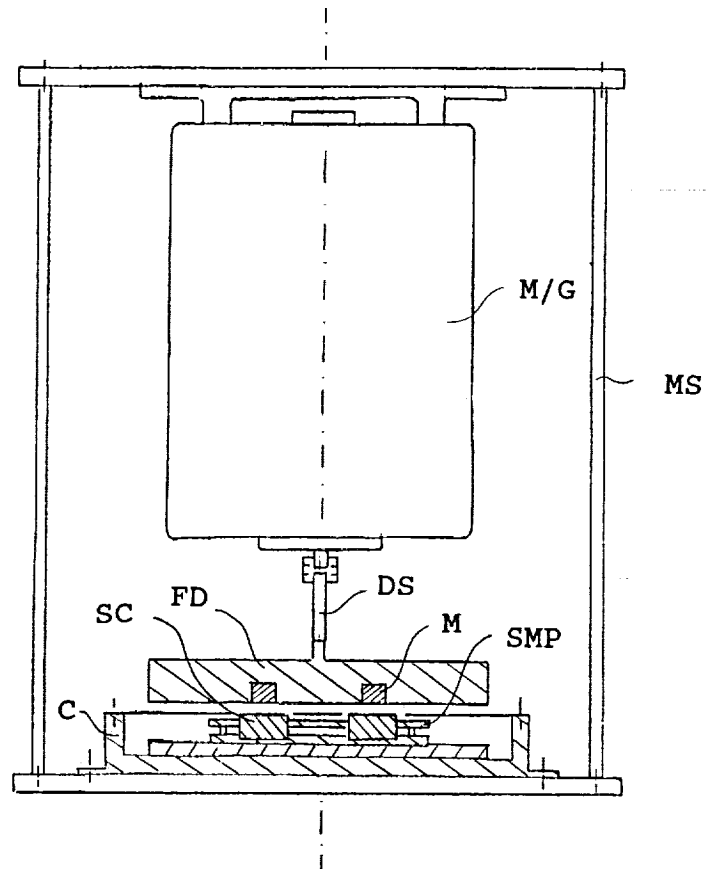plate and Nd-Fe-B magnet. Bottom: Aluminum
flywheel disk.

Figure 5: Schematic of the flywheel system.
C: cryostat, SC: YBCO pellet, FD: flywheel disk
DS: driveshaft with couplings, M: magnet,
SMP: sample mounting plate, M/G: motor/generator
MS: mounting structure